



Evidence of depolymerisation of amorphous silica at medium- and short-range order: XANES, NMR and CP-SEM contributions

L. Khouchaf^{a,*}, A. Hamoudi^a, P. Cordier^b

^a Centre de Recherche de l'Ecole des Mines de Douai, 941, rue Charles Bourseul, BP. 10838, 59508 Douai, France

^b Laboratoire de Structure et Propriétés de l'Etat Solide, UMR 8008 USTL UFR de Physique, Bat C6 59655, Villeneuve d'Ascq Cedex, France

ARTICLE INFO

Article history:

Received 16 June 2008

Received in revised form 7 January 2009

Accepted 27 February 2009

Available online 13 March 2009

Keywords:

SiO₂

Degradation

CP-SEM

XANES

NMR

ABSTRACT

This work reports medium- and short-range order of changes of amorphous silica submitted to chemical degradation. Structural changes were studied, using X-ray absorption near edge structure (XANES), nuclear magnetic resonance ²⁹Si NMR-MAS and controlled pressure scanning electron microscope (CP-SEM). The depolymerisation of amorphous SiO₂ compounds mainly induces the formation of Q₃ species and alkali-rich domains. The XANES Si K-edge spectra demonstrate the presence of different environments of silicon: one with four oxygen atoms and the other with a number of oxygen lower than four in agreement with previous studies.

© 2009 Published by Elsevier B.V.

1. Introduction

Silica is most widely studied because of its technological importance in several disciplines. SiO₂ nanoparticles were used to improve creep resistance of thermoplastic polymers [1]. Natural SiO₂ is used as an aggregate in composite materials such as concrete [2]. The degradation of concrete depends on the crystalline quality of the aggregate. The reactivity of SiO₂ depends on the chemical process that occurs between amorphous or poorly crystallized SiO₂, present in the mineral aggregates called alkali silica reaction (ASR) [3,4].

In fact, alpha quartz (α -SiO₂) with a good structural order and without defects and impurities has a very low reactivity [5,6]. The quartz is thermodynamically more stable, than the silica polymorphs such as tridymite, cristobalite and moganite [5].

Micro-XANES, micro-fluorescence experiments have been carried out to investigate the local structural evolutions of a heterogeneous and natural SiO₂ submitted to ASR process [7]. Using the micro-beam sources, micro-zones with different properties have been separated. Compared to elemental maps obtained by ESEM, micro-X-ray fluorescence (micro-XRF) showed the diffusion of potassium inside the grains more accurately. Si K-edge XANES spectra enabled to follow the dissolution of the grain from the outside to the inside. Potassium K-edge XANES spectra show no

significant changes around K cations from the outside to the inside of the grain. The breaking of Si–O–Si bonds may be attributed to potassium cations. Some questions remain unanswered such as the contribution of each structural phase (crystalline, disordered and amorphous).

Previous studies on the ASR in the natural flint [6,8,9] have shown that the reaction begins with the breaking of bridge siloxane Si–O–Si and formation of amorphous and nanocrystalline phase. However, the presence in flint of different structural areas, such as crystallized, poorly crystallized and amorphous domains makes the study of the mechanism of degradation and the kinetics of the reaction more complex. However, up to now, there has been no published report on the reactivity of amorphous SiO₂ including medium- and short-range order.

In this work we will follow the amorphous silica a-SiO₂ as a model and starting material in order to obtain information about the mechanism that is established in amorphous phase.

2. Materials and methods

The starting material used in this study is a synthetic amorphous silica a-SiO₂ powder from Alpha Aesar with high purity (99.9%) and the average grain size showed two maxima, at 3 and 22 μ m.

Amorphous silica has been submitted to ASR following the protocol below: 1 g of silica powder is introduced in a closed stainless steel container with a mixture of 0.5 g of portlandite Ca(OH)₂. After 30 min of preheating, 10 ml of potash solution KOH (0.79 mol/l) was added to the mix SiO₂ and Ca(OH)₂, and placed under magnetic

* Corresponding author. Tel.: +33 3 27 71 23 19.

E-mail address: khouchaf@ensm-douai.fr (L. Khouchaf).

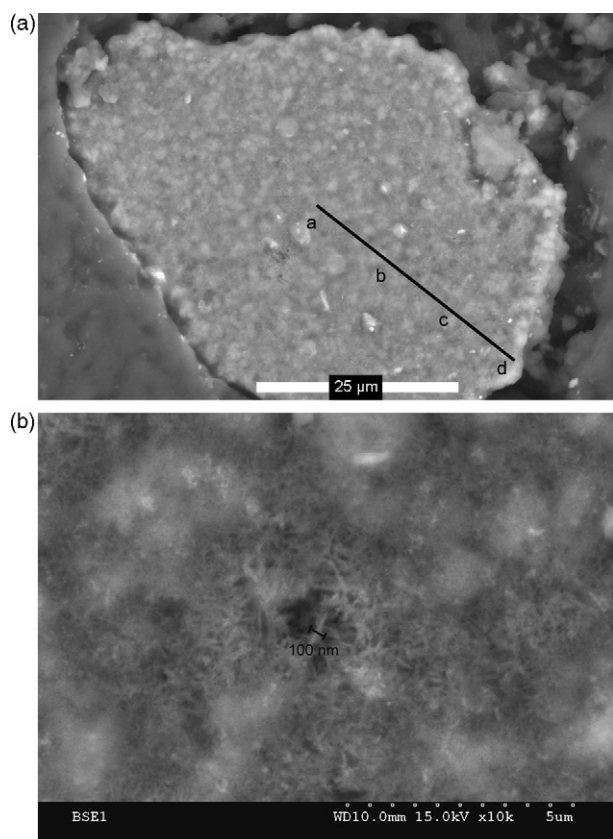


Fig. 1. (a) CP-SEM micrograph of the reacted silica $r\text{-SiO}_2$ (backscattered electrons, BSE). (b) Micrograph of the needles obtained after the reaction (backscattered electrons, BSE).

stirrer to produce homogeneous slurry. The development of the ASR occurs during heating of the autoclave with our mixture at 80°C for 312 h. After this period of reaction, ASR-products were obtained (called $r\text{-SiO}_2$).

Controlled pressure scanning electron microscope (CP-SEM) observations were carried out at accelerating voltage of 15 kV and a probe current of 130 pA using a FEG CP-SEM "Hitachi S4300 SE/N". Observations were performed under vacuum pressure of 0.37 Torr. Low pressure gas (air) is introduced inside the analysis chamber in order to avoid coating operation. The influence of the interaction between electron beam and gas on imaging and microanalysis results was controlled carefully [8,10,11].

XRD spectra were recorded for 2θ values between 10° and 100° with steps of 0.007° and a counting time of 10 s per step using a Bruker D8 Advance diffractometer operating at 40 kV and 40 mA with Co radiation ($\lambda \approx 1.78897 \text{ \AA}$). The original powder has been

introduced into Al_2O_3 cup which was maintained under rotation during the experiment.

X-ray absorption near edge structure (XANES) experiments were carried out on the LUCIA beam line at the Swiss light source (SLS) [12]. The high brightness of synchrotron radiation leads to obtain data with good quality from micro-zones of heterogeneous materials. Micro-XANES spectra at Si K-edge, were recorded using a double crystal monochromator with a $\text{InSb}(111)$ crystal. Spectra were recorded, at room temperature, under high vacuum (10^{-5} Torr) in total electron yield (TEY) mode on a grain embedded in epoxy resin.

^{29}Si magic-angle spinning (MAS) NMR spectra were recorded at room temperature using a Bruker Avance 100 NMR spectrometer with field of 2.34 Tesla. ^{29}Si MAS experiments operating at 19.89 MHz were performed with a 7 mm MAS probe with ZrO_2 rotor at a spinning rate of 4 kHz. Tetramethylsilane (TMS) was used as a reference for chemical shifts measurements. Spectra were recorded with a pulse angle of $\pi/5$ and a recycle delay of 80 s, which enable relaxation. The number of scans was 256 for each sample.

3. Results

Fig. 1a displays a micrograph obtained by CP-SEM with backscattered electrons detection of $r\text{-SiO}_2$. Important modifications are produced after the reaction. Heterogeneous morphology shows the traces of the reaction. At high magnification, disordered needles nanometric sizes (~ 100 nm) are observed (Fig. 1b).

X-ray elemental maps have been performed (Fig. 2) in order to follow the distribution of different cations inside the silica. The later show a heterogeneous aspect of the attack. X-ray elemental maps of silicon Si, calcium Ca, and potassium K show that Ca and K are present on almost all parts of the grain.

X-ray absorption near edge structure, unlike X-ray diffraction, can be used both for crystalline and amorphous materials and gives information on medium-range order. In Fig. 3a are shown the XANES spectra of $a\text{-SiO}_2$ and $\alpha\text{-SiO}_2$ used as a reference. A main peak (A) located at 1846.8 eV and a broad peak (E) located at 1865 eV are present in both samples. Besides, three peaks B, C and D are present in $\alpha\text{-SiO}_2$ XANES spectrum only.

Absorption spectra at Si K-edge at different zones of the $r\text{-SiO}_2$ grain (from the inside to outside, Fig. 1a) were recorded using a micro-beam delivered by synchrotron radiation facility. In Fig. 3b are shown XANES spectra of the $r\text{-SiO}_2$ at different points of the grain compared to $a\text{-SiO}_2$. The energy position of peak A called white line remains unchanged (1846.8 eV) whatever the analyzed zone. Besides, its intensity decreases from the inside to the outside. A second peak f around 1843 eV appears in the degraded silica. The intensity of this peak increases from the inside to outside of the grain in an opposite way compared to the peak located at 1846.8 eV.

The MAS solid-state ^{29}Si NMR spectrum of the starting silica are shown in Fig. 4a. We interpret the NMR spectra using the standard Q_n nomenclature. In this nomenclature the Q_n identifies the con-

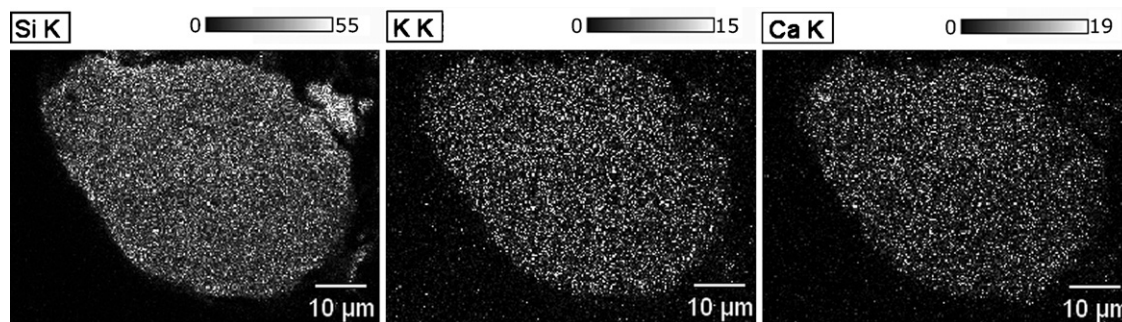


Fig. 2. X-ray elemental maps of Si, K and Ca.

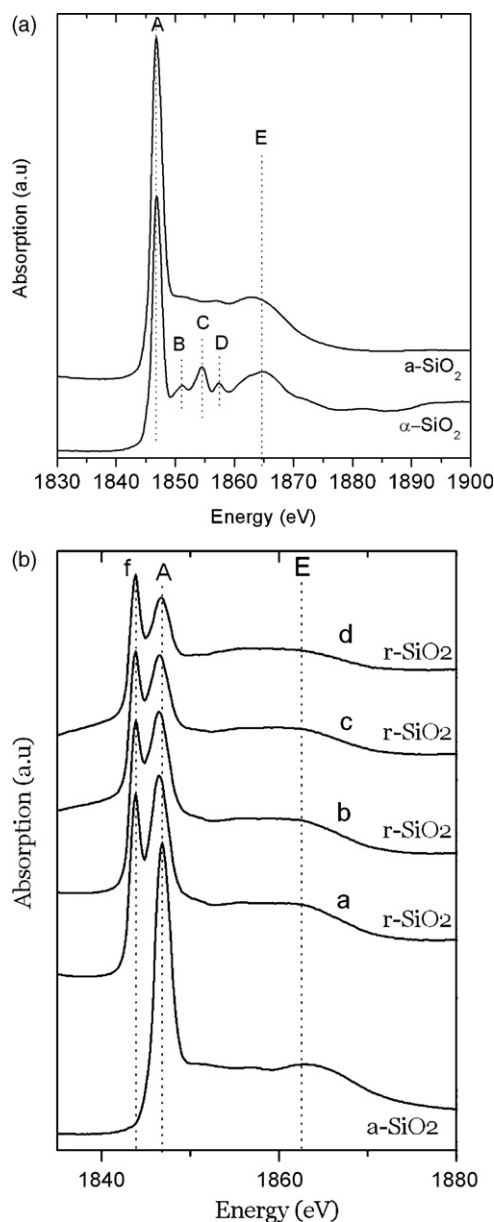


Fig. 3. (a) XANES spectra at Si K-edge of the references: amorphous silica (a-SiO₂) and alpha-quartz (α-SiO₂). (b) XANES spectra at Si K-edge of r-SiO₂ at different zones (a–d as indicated in Fig. 1a) in the grain compared to the starting a-SiO₂.

nectivity of silicate tetrahedron, with n is the number of associated bridging oxygen's (Si–O–Si). These lines can be identified according to literature data with the different tetrahedral Q_n environments of Si in silicates [13]. Fig. 4a shows a signal centred at -110 ppm, attributed unambiguously to Q_4 units in the amorphous silica [14]. The width of this resonance indicates a broad distribution of Si–O–Si angles, which is synonymous with a disordered structure.

Several resonances appear when the reaction proceeds (Fig. 4b), at -90 , -85 and -79 ppm and attributed to Q_3 , Q_2 and Q_1 units, respectively [13–15]. The Q_4 peak corresponding to amorphous silica has totally disappeared.

4. Discussion

We have shown in a recent study [7], that the heterogeneity and the structural state of the SiO₂ compounds play a substantial role in the mechanism of the degradation. Only potassium diffuses inside the grain while the calcium remains outside the grain at

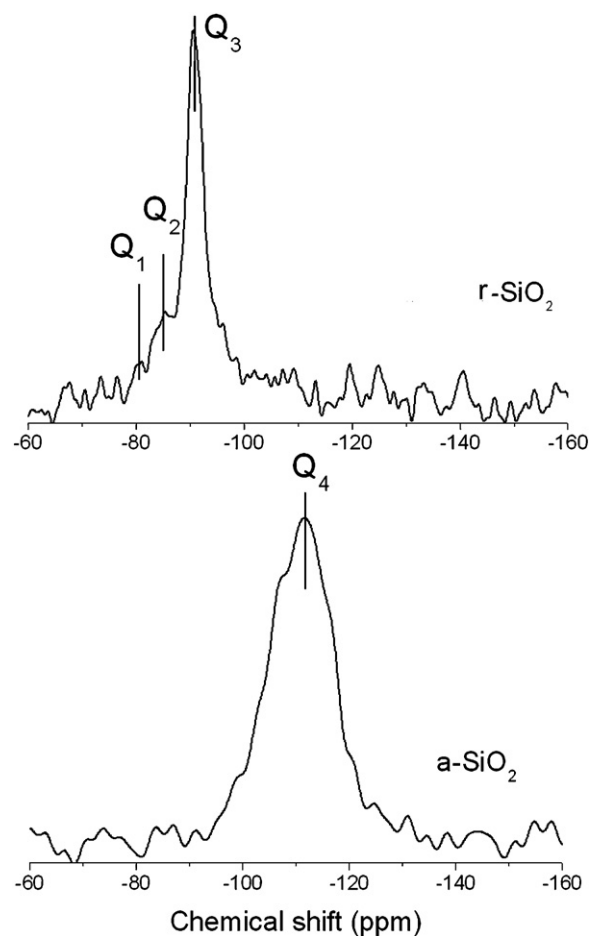


Fig. 4. (a and b) ²⁹Si MAS NMR spectra of r-SiO₂ compared to a-SiO₂.

the beginning of the reaction. In the present work, the penetration of Ca and K in all parts of the grain indicates that the portlandite Ca(OH)₂ is totally consumed by the ASR. The heterogeneity of the attack induces different ratio Ca/Si (less than 0.6) depending on the zone analyzed. The total consumption of portlandite by the reaction involves the formation of relatively stable phases in our samples. This makes information obtained with analysis of the local order more pertinent. These phases were identified by XRD as calcium silicate hydrate (C–S–H). The peaks largely match the ICDD card file numbers 83–1520, 34–0002, and 06–0453.

Based on their form and morphology, disordered needles nanometric size (~ 100 nm) observed in Fig. 1b are attributed to calcium silicate hydrated phases (C–S–H) as indicated in a previous study [16]. The C–S–H compounds are highly complex, and with widely varying composition with amorphous and nanocrystalline behaviour.

The reaction affects the Si–O–Si bonds [6,7]. Complementary information about the evolution of the short- and medium-range order around silicon atoms is obtained from ²⁹Si NMR. Several broad peaks can be observed, typical of a distribution of isotopic chemical shift values caused by structural disorder. The reaction induces depolymerisation of the SiO₂ network, thus, creates Q_3 species consists of the sheet silicate structure, Q_2 species (on SiO₄ tetrahedra in the middle of silicate chains) and Q_1 (tetrahedral in the end of silicates chain).

XANES technique gives information about the medium-range order during depolymerisation process of SiO₂ compounds. It has been established that the various energy resonances above the edge are a signature of the presence of environment with a different degree of coordination for silicon atoms [9,17,18].

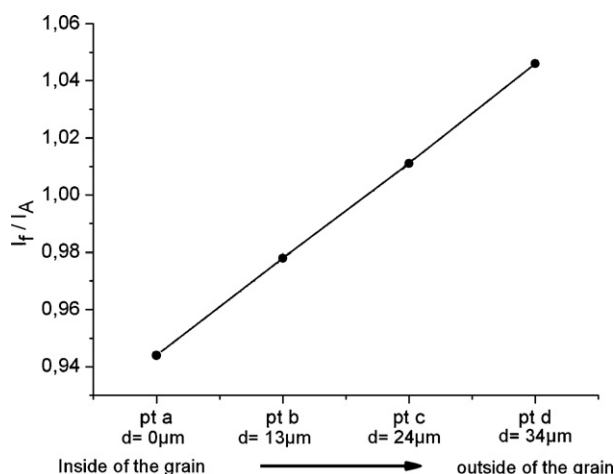


Fig. 5. Evolution of the intensity ratio of the f to A peak deduced from XANES spectra.

The resonances (B–D) observed in Fig. 3a, have been described in previous studies [8,9,11], they are characteristic of crystalline SiO₂ (quartz). XANES spectra of the r-SiO₂ at different points of the grain compared to starting a-SiO₂ show that all spectra present a peak at 1846.8 eV (with a shift of 0.4 eV), which is associated with the electronic transitions of the 1s to 3p state and attributed to tetrahedral environment around the silicon [9]. However, a second peak around 1843 eV appears in the degraded silica r-SiO₂ only. The intensity of this peak increases from the inside to outside of the grain. The origin of this peak may be explained by the presence of silicon atoms surrounded by a number of oxygen lower than four [19,20]. Both XANES and NMR show strong modifications of the SiO₂ network at different scales. The ratio between both environments of silicon obtained by XANES (Fig. 3b) is shown in Fig. 5.

It is clearly demonstrated that the contribution of a silicon environment with a number of oxygen lower than four increases from the inside to the outside. Unfortunately this information cannot be obtained by NMR results dominated by bulk contribution. The absence of the peaks B–D in r-SiO₂ indicates that no medium-range order is present after the reaction.

5. Conclusions

Medium- and short-range order of amorphous silica submitted to chemical stress is followed by CP-SEM, XANES, and NMR techniques. The diffusion of calcium and potassium inside the structure of a-SiO₂ is evidenced. XANES and NMR analysis show that a-SiO₂ tetrahedrons, which form the starting silica network, are mostly affected. Micro-XANES spectra show the presence of a mixture of environments of silicon with four oxygen atoms and with a number of oxygen lower than four. The increase of the contribution of the environment of silicon with a number of oxygen lower than four from the inside to the outside is observed. NMR results show that principally Q₃ and Q₂ species are formed after the depolymerisation of the predominantly Q₄ species present in the starting amorphous SiO₂.

Acknowledgments

X-ray absorption experiments were performed at the Swiss Light Source, Paul Scherrer Institut, Villigen, Switzerland. It was approved by the advisory committee. The authors thank the EC for financial support and Dr. A.M. Flank for his help during synchrotron radiation experiments. The authors thank also Pr L. Montagne for his help and discussion in NMR experiments.

References

- [1] T.H. Zhou, W.H. Ruan, J.L. Yang, M.Z. Rong, M.Q. Zhang, Z. Zhang, A novel route for improving creep resistance of polymers using nanoparticles, *Composites Science and Technology* 21 (2007) 539.
- [2] T. Ichikawa, M. Miura, Modified model of alkali-silica reaction, *Cement and Concrete Research* 37 (2007) 1291.
- [3] L.S. Dent Glasser, N. Kataoka, The chemistry of alkali-aggregate reaction, in: *Proceeding of the 5th ICAAR, Cape Town (South Africa)*, National Building Research Institute of CSIR, 1981, p. 7.
- [4] S. Chatterji, N. Thaulow, Some fundamental aspect of alkali-silica reaction, in: Berube, et al. (Eds.), *Proceeding of the 11th International Conference in Alkali-Aggregate Reaction in Concrete*, Quebec, Canada, 2000, p. 21.
- [5] M.A.T.M. Broekmans, The quality of quartz and its susceptibility for ASR, *Materials Characterization* (53/2-4), Special Issue (29) (2004) 129.
- [6] L. Khouchaf, J. Verstraete, Multi-technique and multi-scale approach applied to study the structural behavior of heterogeneous materials: natural SiO₂ case, *Journal of Materials Science* 42 (2007) 2455.
- [7] L. Khouchaf, F. Boinski, M.H. Tuilier, A.M. Flank, Characterization of heterogeneous SiO₂ materials by scanning electron microscope and micro fluorescence XAS techniques, *Nuclear Instruments and Methods B* 252 (2006) 333.
- [8] L. Khouchaf, F. Boinski, Environmental scanning electron microscope study of SiO₂ heterogeneous material with helium and water vapor, *Vacuum* 81 (2007) 599.
- [9] L. Khouchaf, J. Verstraete, R.J. Prado, M.H. Tuilier, XANES, EXAFS and RMN contributions to follow the structural evolution induced by alkali-silica reaction in SiO₂ aggregate, *Physica Scripta* T115 (2005) 552.
- [10] L. Khouchaf, J. Verstraete, X-ray microanalysis in the Environment scanning electron microscope (ESEM): small size particles analysis limits, *Journal de Physique IV* 12 (2002) 341.
- [11] L. Khouchaf, J. Verstraete, Electron scattering by gas in the environmental scanning electron microscope (ESEM): effects on the image quality and on the X-ray microanalysis, *Journal de Physique IV* 118 (2004) 237.
- [12] A.M. Flank, G. Cauchon, P. Lagarde, S. Bac, M. Janousch, R. Wetter, J.M. Dubuisson, F. Langlois, M. Idir, T. Moreno, D. Vantelon, LUCIA, a microfocus soft XAS beamline, *Nuclear Instruments and Methods B* 246 (1) (2006) 269.
- [13] R.J. Kirkpatrick, MAS NMR spectroscopy of minerals and glasses, in: F.C. Hawthorne (Ed.), *Spectroscopic Methods in Mineralogy and Geology*, vol. 18, 1988, p. 341.
- [14] X.D. Cong, R.J. Kirkpatrick, S. Diamond, Silicon-29 MAS NMR spectroscopic investigation of alkali silica reaction product gels, *Cement & Concrete Research* 23 (1993) 811.
- [15] X.D. Cong, R.J. Kirkpatrick, ²⁹Si MAS NMR study of the structure of calcium silicate hydrate, *Advanced Cement Based Materials* 3 (1996) 144.
- [16] J. Minet, Synthèse et caractérisation de silicates de calcium hydrates hybrides, PhD thesis, Université Paris XI, Orsay France, 2003.
- [17] Li. Dien, G.M. Bancroft, M. Kasrai, M.E. Fleet, X.H. Feng, K.H. Tan, B.X. Yang, High-resolution Si K- and L_{2,3}-edge XANES of α quartz and stishovite, *Solid State Communication* 87 (7) (1993) 613.
- [18] Li. Dien, G.M. Bancroft, M. Kasrai, M.E. Fleet, R.A. Secco, X.H. Feng, K.H. Tan, B.X. Yang, X-ray absorption spectroscopy of silicon dioxide (SiO₂) polymorphs; the structural characterization of opal, *American Mineralogist* 79 (1994) 622.
- [19] V. Belot, R.J.P. Corriu, D. Leclercq, P. Lefèvre, P.H. Mutin, A. Vioux, A.M. Flank, Sol-gel route to silicon suboxides. Preparation and characterization of silicon sesquioxide, *Journal of Non-Crystalline Solids* 127 (1991) 207.
- [20] A.M. Flank, R.C. Karnatak, C. Blancad, J.M. Esteve, P. Lagarde, J.P. Connerade, Probing matrix isolated SiO molecular clusters by X-ray absorption spectroscopy, *Zeitschrift der Physik, Reihe D: Atoms, Molecules and Clusters* 21 (1991) 357.